



16th World Conference on Earthquake Engineering, 16WCEE 2017

Santiago Chile, January 9th to 13th 2017

Paper N° 3312

Registration Code: S-S1454548818

CYCLIC PERFORMANCE OF SHEAR LINKS WITH CONTACT STIFFENERS

D. Volynkin⁽¹⁾, G. C. Clifton⁽²⁾, P. Dusicka⁽³⁾

⁽¹⁾ PhD Student, The University of Auckland, dmitry.volynkin@auckland.ac.nz

⁽²⁾ Associate Professor, The University of Auckland, c.clifton@auckland.ac.nz

⁽³⁾ Associate Professor, Portland State University, dusicka@pdx.edu

Abstract

Shear yielding links are widely used as seismic energy dissipation components in eccentrically braced frames, linked column frames and in coupled shear walls. Typically, shear links are strengthened with intermediate stiffeners welded to the web. The stiffeners are useful in delaying the onset of buckling and associated failure modes as the shear link is cycled with increasing inelastic deformations. However, these intermediate stiffeners have been shown to be a source of early fracture initiation in the web at the stiffener to web welds. The typical mode of failure of shear links that do not exhibit web buckling is a web fracture that initiates near the stiffener welds. This paper examines the possibility of not welding the intermediate stiffeners to the web (ie welded only to the flanges) and instead to rely on the contact interface between the stiffener and the web; with pairs of stiffeners placed at each location to suppress web buckling out of plane in both directions. Large scale experiments were conducted on two links, one with stiffeners conventionally welded and another with flange welded only contact stiffeners. The links consisted of 42in long W14x48 sections stiffened on both sides by stiffeners that dimensionally conformed to AISC specifications. Both links exhibited stable hysteresees. The rotation at which the strength of the link with contact stiffeners degraded was 0.114 rad, well above the 0.090 rad achieved by a conventionally welded link. The contact stiffeners also reduced the overstrength developed by the active link under high shear demand. These positive outcomes indicate the potential for adoption of contact stiffeners for design, the procedures of which would only require minor modifications to fabrication procedures and minor implications on cost. For larger wide flange links, code requirements dictate the use of stiffeners on both sides of the web, in any case, meaning cost neutrality.

Keywords: shear links; replaceable bolted active links; eccentrically braced frames; full-scale; overstrength



1 Introduction

EBFs are a widely used steel seismic resisting system, due to their combination of high elastic stiffness and high ductility. Typically, a link classified as a short shear link is used as the yielding element. EBFs were developed primarily in the work by Popov in the 1970s and 1980s, with the overall behavior and design summarized by Popov, Kasai & Engelhardt (1986). This Introduction describes the recent developments in shear link design as well as summarizing recent trends in research.

There have been a number of recent developments in the link's material and geometrical proportions, such that the design equations, for the stiffener spacing, have been revisited by this paper's authors. As part of this revisitation, shear links without stiffeners and shear links without stiffener web welds were experimentally tested and analyzed.

The original stiffener spacing provisions were based on achieving a web panel size such that, at a certain rotation, the shear link does not buckle. In order to do this, intermediate stiffeners were welded to flanges and webs in order to create smaller web panel sizes. The issue with this approach has been that the stiffener welds themselves typically were the starting points for shear links to have their fractures initiate at (as seen in work by Okazaki 2005). Furthermore, adding more stiffeners than necessary is deemed conservative, however, if the detrimental effects of the stiffener web weld are recognized then over prescribing stiffeners reduces the ultimate rotation that the stiffener may attain. This was seen in the built up shear link work by this paper's main author (2016 REF), where links with stocky webs not requiring stiffeners performed better without them.

The current stiffener spacing equation is $s = 30t_w - 0.2d$ (AISC, 2005) and it was derived from the work developed by Kasai & Popov (1986). It was based on highly variable ASTM A36 steel, which today is not used in seismic applications in favor of ASTM A992 steel or equivalent for rolled sections.

Throughout the testing history of shear links, the loading protocol was not standardized, with each researcher using their own protocol. There was no de-facto protocol before 2002 and, since 2002, a number of studies have used their own loading protocol. More recently a rationally based EBF seismic loading protocol has been produced (Richards & Uang, 2003, published as AISC2005), which is less stringent than the 2002 protocol. The A992 steel under the 2005 protocol has performed noticeably better than the 2002 protocol (particularly in work by Okazaki, 2005) in terms of the maximum ductility reached. Hence for this study, the AISC2005 protocol was selected.

Built-up shear links are increasingly presented in research (e.g. Itani, Elfass & Douglas, 2003; McDaniel, Uang & Seible, 2003) and used in practice, as they are more flexible in terms of design as opposed to rolled sections which may not have been derived specifically for use as shear links. From past research, they have performed exceptionally well, to the point of fracturing at the stiffener to web weld without buckling. This prompted a re-think of whether a stiffener is even required (Dusicka, 2010).

Furthermore, increasing numbers of links have become bolted shear links (for instance, in the work by Stratan & Dubina, 2004; Dubina, Stratan & Dinu, 2008; Mansour 2010; and incidentally by Okazaki, 2005) with the yielding taking place inside the link only, with the endplate connection and the supporting structure remaining elastic. This places greater ductility demand on the link itself as the inelastic action cannot spread to the collector beam as currently allowed under the AISC, NZS and other provisions worldwide. This bolted replaceable EBF active link has now become standard practice in New Zealand (Clifton & Cowie, 2013) following the excellent performance of EBF systems in the devastating 2010/2011 Canterbury earthquake series.

Work done by Stephens (2015), showed the potential for continuously stiffened links. In that study, the link webs were continuously restrained by sandwiching the webs in between layers of neoprene. The study herein, builds on that idea by using a number of contact stiffeners along the web, in order to restrain the web without mechanically attaching it to any points that would move independently of the web. Typically, shear links are strengthened with intermediate stiffeners welded to the web. These are useful in delaying the onset of buckling as

the shear link experiences larger and larger deformations. However, they prevent the web from smoothly deforming past the connecting welds and thus cause strain concentrations leading to early fracture initiation. Past research has shown that the typical mode of failure is a fracture that initiated near the stiffener welds if the link had not buckled prior. This was the case, for example, in the experiments by Okazaki *et al.* (2005).

2 Experimental Test Set Up

The test setup consisted of a full scale D-Braced Eccentrically Braced Frame (D-EBF), see Fig. 1. It was fabricated out of wide flange rolled sections, with W360X71 [W14X145] for the columns, a W610X113 [W24X76] collector beam and a W400X101 [W16X68] brace section. The actuator was attached at the highest point possible to maximize the available shear force in the active link. The shear in the link was derived from the setup geometry: $V_{link} = P \times (H/L) = P \times 1.156$ where P is the load as measured by the actuator load cell. Centerline dimensions H and L are in Fig. 1. Similar calculations are described by Dusicka *et al.* (2010) and McDaniel *et al.* (2003). The bottom column to floor connections were pinned and lateral supports were provided at active link level on each of the columns. No lateral supports were provided directly to the ends of the active link away from the column or collector beam.

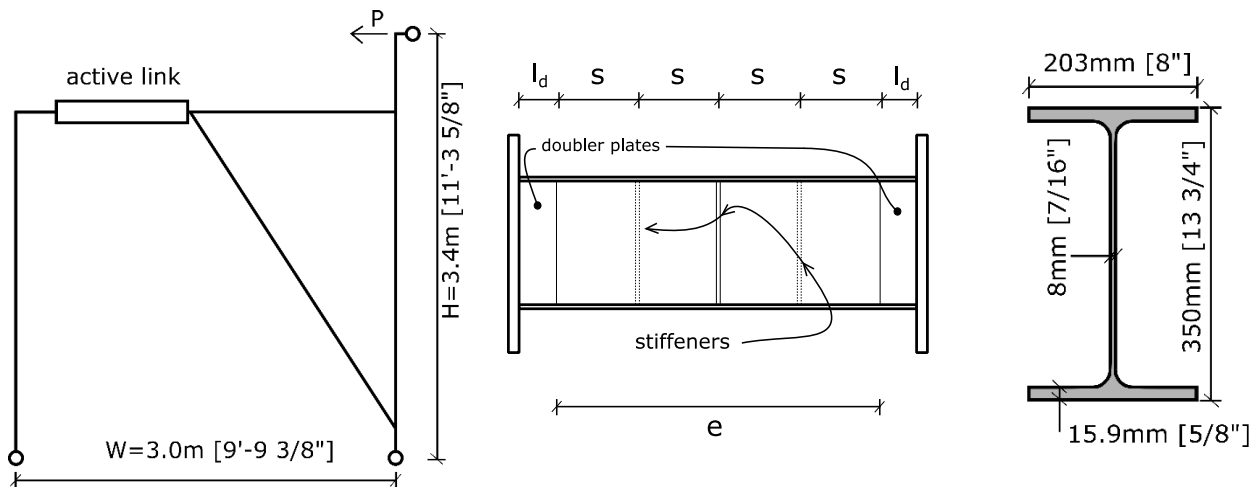


Fig. 1. EBF Test setup and dimensions; Active link key dimensions; Link section W360X71 [W14X48]

The active links were connected into the D-EBF via a bolted connection, with an 8xA490 bolt connection for the W360X71 [W14X48] links and a 16xA325 bolt connection for the BU links on each side, described in the next section.

The loading regime was as described by Richards & Uang (2003) in their technical report and later adopted by AISC in 2005 as a shear link loading protocol. A number of cycles are prescribed, with the latter steps increasing in magnitude by 0.02 radians per step until link failure. It is not prescribed in AISC2005 how much strength degradation is permissible before the specimen is deemed a failure, nor was it ever formally stated in any of the previous studies, except by Stephens (2014). Thus a 20% degradation from the maximum shear strength so far attained was used as a failure criteria. It should be noted that in deriving this protocol, the damage parameter is exponentially larger with increases in rotation. That is, the increase in damage parameter for a link rotating from the ± 0.09 rad cycle to the ± 0.11 rad cycle is much greater than the increase for a link rotating from the ± 0.07 rad to the ± 0.09 rad cycle.

The shear link rotation angle was measured and calculated in the same way as by McDaniel *et al.* (2003), with threaded rods tack welded in the middle of the flange thickness ($b = d - t_f$) and the inside dimension e was taken as the link length ($a = e$), because the deformation was primarily concentrated in this region. This was

confirmed with hysteretic data that measured very small amounts of rotations in the doubler plate regions as well as a lack of white wash flaking in said region throughout all the tests. Diagonal Linear Variable Differential Transformers (LVDTs) were used to measure the changes in diagonal length (c_1 and c_2) so that the total rotation angle could be computed from $\gamma = (c_1 - c_2) / (a^2 + b^2)^{0.5} / (2ab)$.

Although the AISC2005 protocol and the measured rotation is stated as a “total” rotation, the qualification of a link depends on attaining a “plastic” rotation angle of $\gamma_p = 0.080 \text{ rad}$. The angle the link made on its first excursion beyond its nominally plastic shear strength value, $V_p = f(F_{y,nominal})$, was taken as the yield angle. It was generally under 0.010 rad and therefore the qualifying load cycle was of magnitude $\gamma = 0.090$. The link was required to perform both the negative and then the positive half cycles for that cycle to be deemed complete.

The link rotation angle was continuously calculated and the loading actuator was directly controlled during the test using a target displacement.

3 Specimens Tested

The relevant links were the baseline link “AL-3S”, the contact stiffener version of that same link with three pairs of contact stiffeners without web welds “AL-3C”, rather than three alternating stiffeners with web welds. Additionally, link “AL-B” was tested as a control, to examine the performance of a link without any stiffeners. The geometrical dimensions of the W360X71 [W148X48] links are detailed in the table below, with key section dimensions in Fig. 1.

Table 1. W360X71 [W14X48] section dimensions and properties.

	d (mm) [in.]	b_f (mm) [in.]	t_w (mm) [in.]	t_f (mm) [in.]	h_w (mm) [in.]	Grade	$F_{y,web}$ (MPa) [ksi]	$F_{u,web}$ (MPa) [ksi]	ϵ_{web}
W360X71 [W14X48]	349 [13.75]	203 [8]	7.9 [0.3125]	15.9 [0.625]	318 [12.5]	A992	364 [52.8]	483 [70.0]	25.05%

Fig 2 illustrates the AL-3C specimen, showing the same number of web stiffeners in terms of spacing, however AL-3C has one on each side of the web, without the web being welded to the stiffener. The different endplate details reflect the different stages in the overall experimental process, where earlier design iterations of endplate connections failed unexpectedly with bolts prying (despite complying with design principles). Thus the later tested AL-3C had a thicker endplate with more bolts. For all links, $s = 216\text{mm}$ [8 ½ in] (except for AL-B), $l_d = 102\text{mm}$ [4 in], with the thickness of the doubler plates at $t_d = 9.5\text{mm}$ [3/8 in].

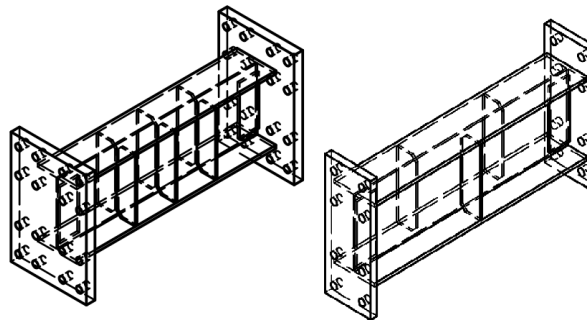


Fig 2. AL-3C (left) specimen sketch compared to the AL-3S (right) baseline link.

4 Experimental Performance

The hysteretic performance of each of the links is summarized in the three curves below:

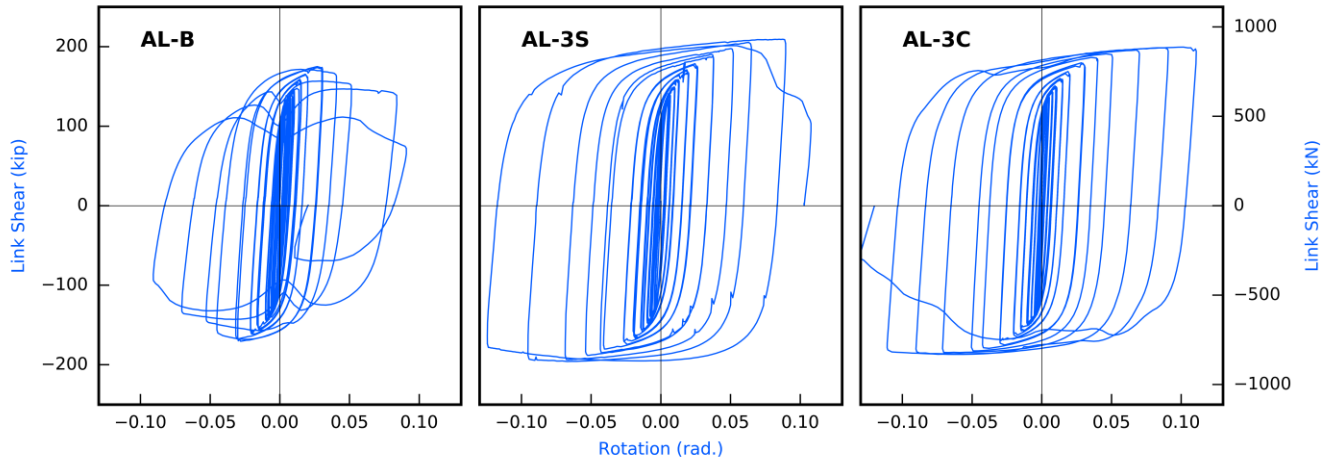


Fig 3. Hysteresis curves for each of the AL-B, AL-3S and AL-3C stiffeners arrangements.

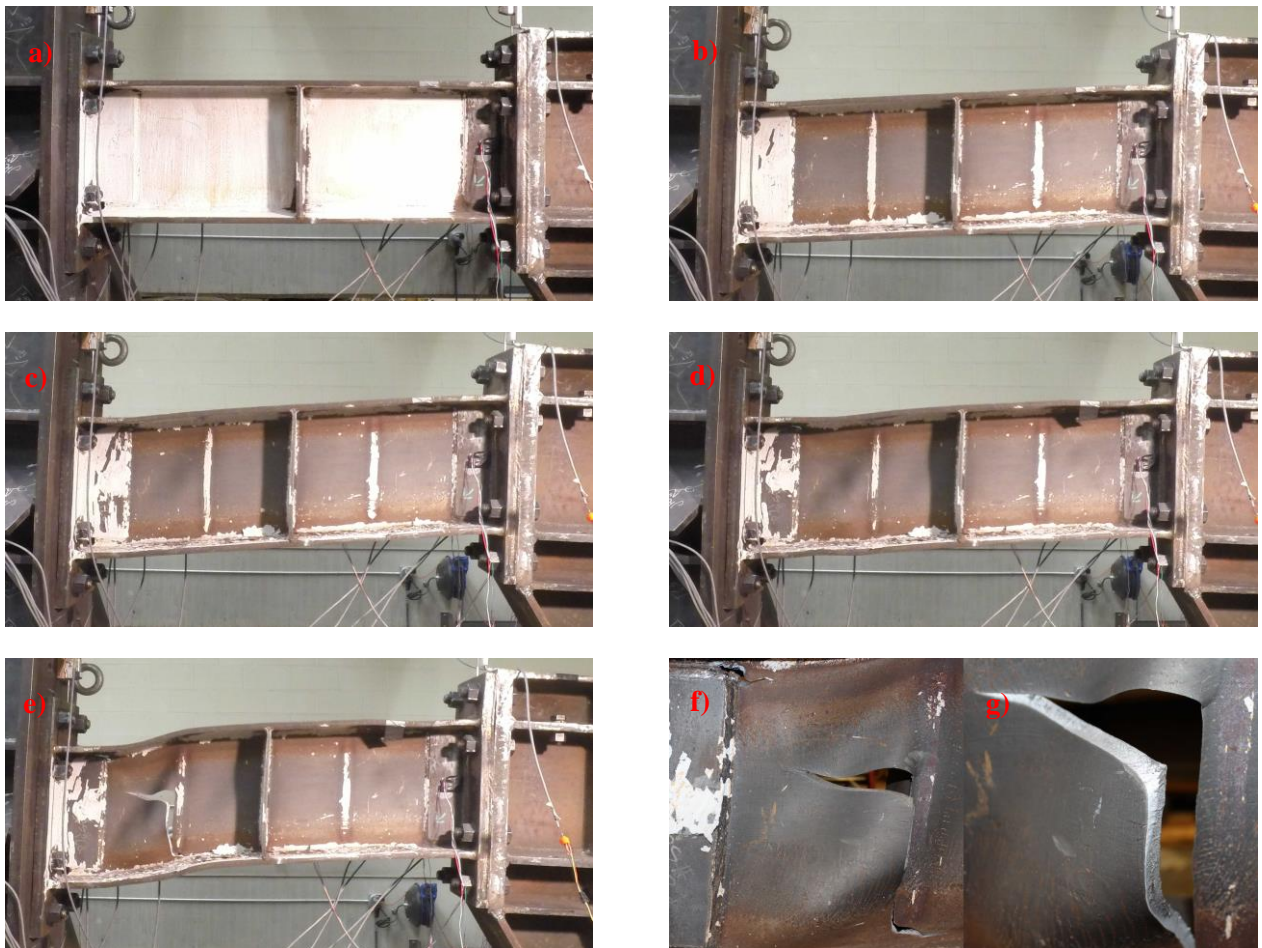


Fig. 4. Link AL-3S at 0.00, 0.07, 0.09 rad, at first fracture, at final fracture and fracture close ups

4.1 AL-3S

Link AL-3S exhibited a stable hysteretic loop right up until the -0.11 rad cycle where it degraded slightly. This was followed by a fracture and load degradation upon attempting to reach $+0.11$ rad (Fig. 4). Photos a) through c) show the link at 0.00 , 0.07 and 0.09 rad respectively. There are signs of buckling in the northernmost (leftmost) panel in photo C. The first signs of vertical cracking along the stiffener are in photo d), with e) showing the final crack pattern. Cracks are also visible near the web doubler plate weld in photo f), however they were away from critical load paths so did not grow or cause issues. Photo g) shows a close up of the fracture and the smooth and shiny surface of the inside of the now exposed web.

4.2 AL-B

The AL-B link had no web stiffeners and was not expected to perform satisfactorily. Early on in the loading protocol, the hysteretic loops exhibited pinching behaviour. This was due to the fact that the entire web panel buckled and upon load reversals it underwent reversals of its buckled shape – thus at the midpoint of this transformation the link had low amounts of shear resistance. Photos A to C show the link at 0.00 , 0.05 and 0.07 rad respectively, with photo D showing the initiation of failure at the $+0.090$ rad cycle. The final X shaped fracture pattern in photo E shows that for each direction of load, the fracture was diagonal in shape. This link had buckled at approximately the 0.0375 rad. cycle, making it unsuitable for most applications.

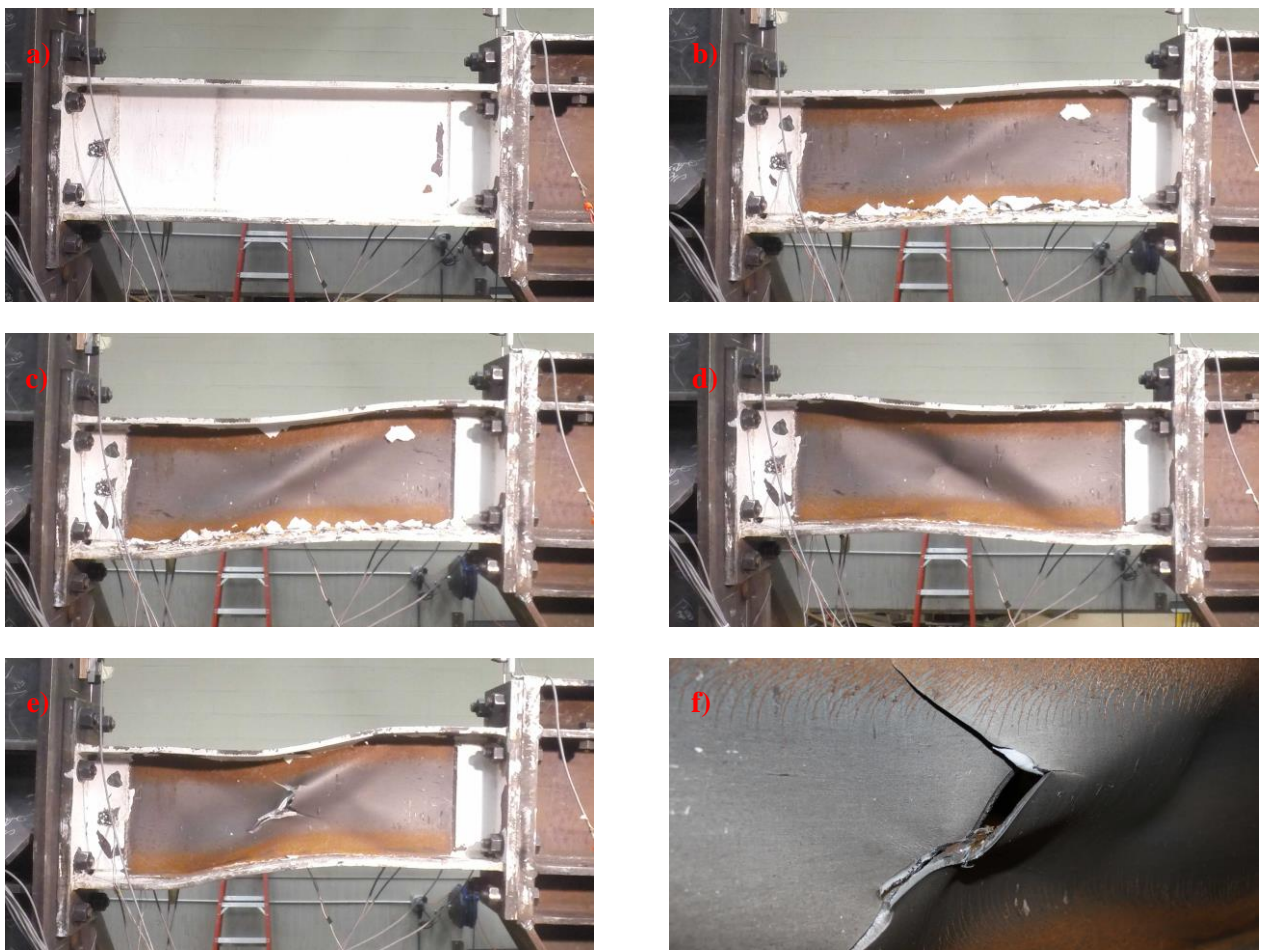


Fig. 5. AL-B with 0.00 , 0.05 , 0.07 rad, initiation of fracture on attempting to reach $+0.09$ rad, final fracture pattern and close up of the final fracture pattern.

4.3 AL-3C

The link exhibited a stable hysteretic performance up until fracture and load degradation (Fig. 6). It deformed in a stable manner with only one half cycle prior to fracture degrading in strength somewhat noticeably. The key points in Fig. 6 c) are as follows. **A:** (γ_e, V_y) The yield point as per the mill certificates in terms of the V_y strength; the rotation at this point was 0.003 rad. **B:** $(\gamma_{V_{max}}, V_{max})$ The maximum attained shear force was 199.4 kip at 0.102 rad. **C:** $(+\gamma_{0.080}, +V_{0.080})$ The criteria rotation of 0.080 radians of plastic rotation was reached on the positive side of the curve at a shear resistance of 198.5 kip. **D:** The first instance of the shear force degrading to below 80% of V_{max} on the positive side of the curve was not attained. **E:** $(-\gamma_{0.080}, -V_{0.080})$ The criteria rotation of 0.080 radians of plastic rotation was reached on the negative side of the curve at a shear resistance of -185.2 kip. **F:** $(-\gamma_{deg}, -V_{deg})$ The first instance of the shear force degrading to below 80% of V_{max} on the negative side of the curve was attained at -0.118 rad and a shear resistance of -148.8 kip. **G:** $(\gamma_{max}, V_{\gamma_{max}})$ The maximum rotation attained anywhere was 0.102 rad at a shear force of 198.5 kip.

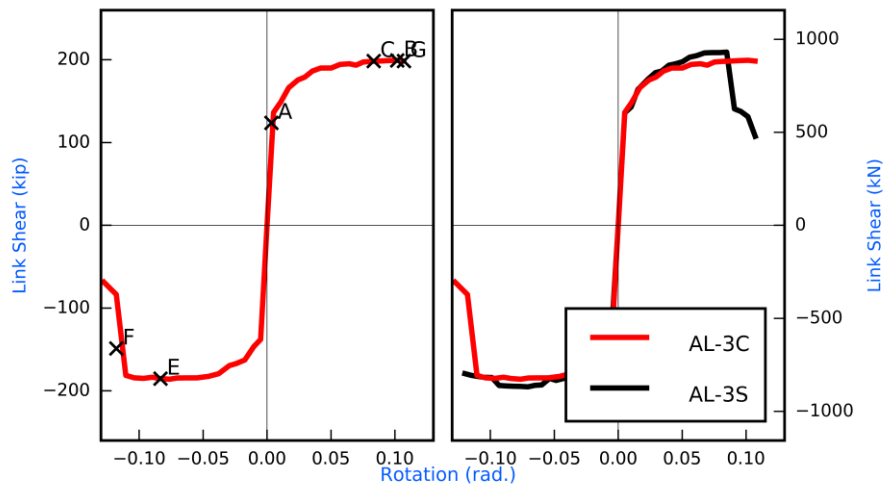


Fig. 6. (Left) AL-3C backbone with key points and (Right) Backbone comparison

The overlaid backbone curves in the bottom right of Fig. 6 show a slightly higher shear force attained during the AL-3S test, suggesting that the use of contact stiffeners allows a smoother deformation and a lower overstrength. Selected photographs from the time lapses taken during testing are presented in Fig. 7. The deformations of links AL-3C and AL-3S are compared here. The photographs show a gradual increase in the rotation angle on the positive (actuator pulling) side of the backbone curve. The whitewash paint had flaked relatively. The final photographs show that the AL-3C link had confined the largest deformations to the inner two panels whilst the AL-3S link had its major buckling and therefore fracture in the left hand panel.

Starting at 0.05 radians of rotation the AL-3C link had some slight buckling, however, unlike a traditional link the buckling looked to be less dependent on whichever panel it was in. This was likely due to the fact that some physical gap existed between the web and the contact stiffeners, meaning that initially the link will deform as if it was a bare link. At 0.07 radians, the buckling was more pronounced and at 0.09 radians, where the link is generally judged to be fit or not, the differences were quite clear. The buckling in AL-3S was confined to one panel region, while the buckling in AL-3C was in two panels with some overlap in terms of how spread the buckled shapes were.

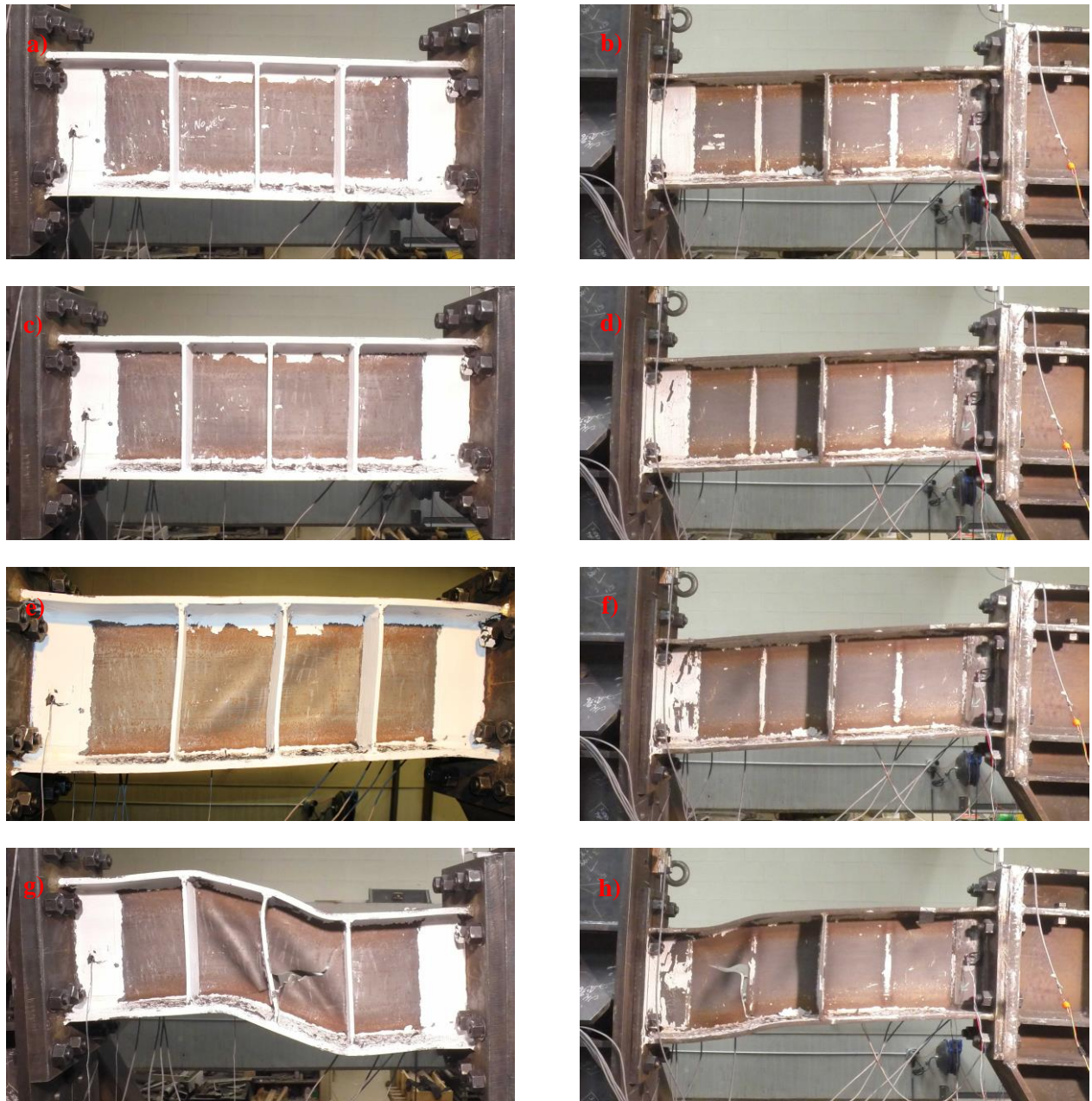


Fig. 7. AL-3C (left) and AL-3S (right) links at selected rotations (0.03, 0.05, 0.09, fracture)

Given that every other non-contact stiffener link had a tendency to buckle and fracture in the panel that happened to experience the most buckling first, the contact stiffeners presented the advantage of allowing the buckling between panels to be shared to a certain extent. This is evident in the last two photographs above where the buckled panels had some continuation between each other in the contact stiffener link. From the experimental notes and close up inspections of the links during and after testing, it was evident that the fractures in the AL-3S case had initiated near the stiffener weld and propagated up the weld and into the buckled shape; whilst the AL-3C link had its fractures initiated due to the tension field in the web being in contact with the stiffeners. The fracture then, in the latter case, travelled in both directions into both panels.



5 Discussion

Links with contact stiffeners behaved just as well, if not better than conventionally stiffened links. The AL-3C link had reached 0.114 radians of deformation before its load carrying capacity had degraded, as opposed to the AL-3S link which had only attained 0.090 rad. The link with contact stiffeners had its web deform more evenly through two panels rather than the conventionally stiffened links which tended to have all their buckling confined to the one panel. This confinement of deformation to the one panel was detrimental as, once buckled at approximately 0.03 to 0.05 rad, the system tended to continue buckling in that one panel, reducing the section’s rotational capacity. Up to a certain rotation, the AL-3C link appears to have behaved much like a bare link, as the web’s buckling was unrestrained for the first few millimetres of its lateral movement. This was because the contact stiffeners can only be so close to the web itself and at smaller rotations the web has not had a chance to make contact with the stiffeners yet. Once the AL-3C link had sufficiently buckled, fractures were initiated by a combination of tension field action in the buckled web as well as friction/contact between the web and the contact stiffeners. Both the AL-3C and AL-3S links exhibited very similar performance characteristics of a stable deformation history, followed by a buckling of the web at larger cycles and then at larger cycles still, the fracture and loss of strength in the web. This suggests that using contact stiffeners did not alter the behaviour of the link adversely or dramatically. Due to the fact that the AL-3C link had effectively larger deforming and buckling panels than the AL-3S link; it is evident that for better link performance it is more important to suppress buckling, rather than to try to reduce individual web panels to smaller sizes. The latter is the approach used by the AISC stiffener spacing equations where each panel’s size is assumed to be the main defining factor in determining the final rotation that the panel may achieve.

Overstrength values are important in determining the magnitude of the actions on EBF elements outside of the link component, so that they may resist the fully strain hardened and yielded levels of shear resistance that the links can attain. The table below utilizes the data taken from all past studies and presents the average overstrength attained for the ASTM A992Gr50 material when used as a shear link. When compared to the overstrength value attained for the AL-3S link, on average the overstrength value is 8% lower at each of the plastic rotation levels. The implication for design of contact stiffeners is that less stringent requirements can be applied to the EBF secondary elements.

Table 2. Overstrength values for the links tested

γ_p	0.02	0.03	0.04	0.05	0.06	0.07	0.08	max	
AL-3S	1.40	1.45	1.48	1.51	1.52	1.54	1.55	1.55	
A992Gr50	1.47	1.54	1.60	1.66	1.69	1.72	1.73	1.67	
	Average								
Decrease	5%	6%	7%	9%	10%	10%	11%	7%	8%

6 Potential Code Provisions

Points in the following paragraph may be taken away from this research for designers. The information available is not enough to justify any amendments to structural building codes. However, at their own risk, engineers may design links using the following points as guidance. No liability is accepted or assumed by the authors or editors of this document.

“An engineer may design the contact links as they would conventionally stiffened links but use pairs of contact stiffeners in place of normal stiffeners. That is, use the same stiffener spacing equations.”

A small cost benefit may be achieved when designing shear links of 635mm [25 in] depth or more, as the current AISC (and worldwide) provisions require double sided links welded to the web at such depths, thus



omission of welds may be more economical. The gap between the link's web and the contact stiffeners should be as small as practicably possible during fabrication, preferably with the stiffener edge in loose contact with the web.

7 Conclusions and Further Research Recommendations

To summarize, a link with contact stiffeners should have no issues with performance. The AL-3C link in this study performed just as well as the conventional link, and exhibited smaller overstrength values than other links made out of the same material. Further research is suggested starting with the following areas:

- Given that only one link was tested with contact stiffeners and compared to a conventional link, further testing is preferable to refine any of the broad generalizations made here. Links at different section sizes and lengths may need to be tested to confirm the behaviour of contact stiffeners across a range of shear links.
- Changing the gap between the contact stiffeners will delay the transition point at which the link stops behaving as a bare link and starts behaving as a stiffened link. A larger gap may be beneficial and may allow greater rotations to be reached. However, this may be difficult to achieve during fabrication without the use of some kind of spacers. Because larger gaps may allow for larger rotations, it may be possible to further relax the stiffener spacing criteria if contact stiffeners are used.

8 Notation Used

A36	[ASTM] Older steel standard, 248MPa [36ksi] minimum specified strength, however the standard is very broad and steels that do not attain the A992 or A507 may be sold as A36, with strengths at 345MPa [50ksi]
A490	[ASTM] Bolt specification, higher yield stress than the more common A325, but less ductile
A992	[ASTM] Common hot rolled steel in the US, typically A992Gr50 [345MPa]
b_f	flange width
d	section height
e	length of link on the inside of the web doubler plates
E	Young's Modulus
e'	clear length of link (inside of endplate to endplate) $e' = e + 2l_d$
F_u	Steel ultimate tensile strength (or minimum specified ultimate tensile strength)
F_y	Steel yield strength (or minimum specified yield strength)
H	height of actuator from pinned base connections
h_w	web height



k_{det}	distance from face of flange to start of k area. In contrast k_{des} is a lower value used for some design calculations, while k_{det} is a higher value typically used conservatively for fabrication tolerance.
L	width of EBF test frame
l_d	web doubler plate length
M_p	Shear link moment capacity
P	actuator force
s	stiffener spacing within e
$s_{\#}$	number of stiffeners
t_d	doubler plate thickness
t_w	section web thickness
V_{link}	shear inside link test specimen
V_p	Shear link shear strength
γ	total link rotation
γ_e	elastic link rotation
γ_p	plastic link rotation
ε	strain (or fracture strain)
φ_{oms}	link overstrength factor

9 Acknowledgements and Disclaimer

This research was jointly funded by the American Institute of Steel Construction (AISC) and New Zealand's Heavy Research Association (HERA). Their contributions are greatly appreciated. The large investment of time and expertise from authors 2 and 3 is also greatly appreciated.

Information in this document is provided as is and no guarantee or liability is assumed by any of the authors or sponsors. Care was taken in preparing this document but whoever decides to use the information contained herein, must understand any limitations of this information and do so at their own risk.

10 References

- [1] AISC. (2005). "Seismic Provisions for Structural Steel Buildings". ANSI/AISC 341-05, Chicago.
- [2] Clifton, G. C. and Cowie, K. (2013) "Seismic Design of Eccentrically Braced Frames", HERA Publication P4001, HERA, Auckland, New Zealand
- [3] Dubina, D., Stratan, A., and Dinu, F. (2008). "Dual high-strength steel eccentrically braced frames with removable links." Earthquake Eng. Struct. Dyn., 37(15), 1703–1720



- [4] Dusicka, P., Itani, A., Buckle, I. "Cyclic Behavior of Shear Links of Various Grades of Plate Steel: Journal of Structural Engineering, Vol. 136, No. 4, April 2010. ISSN 0733-9445/2010/4-370–378. DOI: 10.1061/(ASCE)ST.1943-541X.0000131.
- [5] Gerard, G., "Critical Shear Stress of Plates above the Proportional Limit," Journal of Applied Mechanics, Vol. 15, No. 1, March, 1948, pp. 7-1 [as cited by Kasai & Popov (1986)].
- [6] Itani, A., Elfass, S., Douglas, B. "Behavior of Built-Up Shear Links Under Large Cyclic Displacement", Engineering Journal, Fourth Quarter, 2003, pp. 221-234.
- [7] Kasai, K., Popov, E. "Cyclic Web Buckling Control for Shear Link Beams" Journal of Structural Engineering, Vol. 112, No. 3, March, 1986, pp. 505-523. ISSN: 0733-9445/86/0003-0505/\$01.00. Paper No. 20451.
- [8] McDaniel, C., Uang, C. M., and Seible, F. "Cyclic testing of built-up steel shear links for the new bay bridge." Journal of Structural Engineering, 129(6), 801–809, 2003
- [9] Mansour, N., Christopoulos, C., Tremblay, R. "Experimental Validation of Replaceable Shear Links for Eccentrically Braced Steel Frames". Journal of Structural Engineering, Vol. 137, No. 10, October, 2011. ISSN 0733-9445/2011/10-1141–1152. DOI: 10.1061/(ASCE)ST.1943-541X.0000350.
- [10] Mansour, N. "Development of the Design of Eccentrically Braced Frames with Replaceable Shear Links", PhD Thesis, 2010, University of Toronto.
- [11] Liu, J., Sabelli, R., Brockenbrough, R., Fraser, T. "Expected Yield Stress and Tensile Strength Ratios for Determination of Expected Member Capacity in the 2005 AISC Seismic Provisions" Engineering Journal, First Quarter, 2007, pp. 15-25.
- [12] Nashid H, Clifton, C, Ferguson, G., Hodgson, M.A., Seal, C.H., Choi, J-H. "Relationship Between Hardness and Plastically Deformed Steel Elements" , Earthquakes and Structures, Vol 8, No 3, 2015, 617-635
- [13] Okazaki, T., Arce, G., Ryu, H., Engelhardt, M. "Experimental Study of Local Buckling, Overstrength and Fracture of Links in Eccentrically Braced Frames" Journal of Structural Engineering, Vol. 131, No. 10, October, 2005, pp. 1526-1535. ISSN 0733-9445/2005/10-1526–1535. DOI: 10.1061/(ASCE)0733-9445(2005)131:10(1526).
- [14] Popov, E., Kasai, K., Engelhardt, D. "Advances in Design of Eccentrically Braced Frames", Presented at the Pacific Structural Steel Conference, Auckland, August 1986. Bulletin of the New Zealand Society for Earthquake Engineering, Vol. 20, No. 1, March 1987.
- [15] Richards, P. "Cyclic Stability and Capacity Design of Steel Eccentrically Braced Frames". PhD Dissertation, University of California, San Diego, 2004.
- [16] Richards, P. Uang, C. "Testing Protocol for Short Links in Eccentrically Braced Frames", Journal of Structural Engineering, Vol. 132, No. 8, August, 2006. ISSN 0733-9445/2006/8-1183–1191. DOI: 10.1061/(ASCE)0733-9445(2006)132:8(1183).
- [17] Steel Structures Standard NZS3404: 1997/2001/2007 Parts 1 (Standard) and 2 (Commentary). Standards New Zealand, ISBN. (Published 1997; revised 2001 and 2007), Wellington, New Zealand.
- [18] Steel Structures Standard NZS3404:Part1:2009. Standards New Zealand. ISBN 978-1-86975-126-5
- [19] Stephens, M., Dusicka, P. "Continuously Stiffened Composite Web Shear Links: Tests and Numerical Model Validation". Journal of Structural Engineering, Vol 140, No. 7, July, 2014. DOI: 10.1061/(ASCE)ST.1943-541X.0000996, 04014040.